

ORIGINAL RESEARCH

Inhaled Carbon Dioxide Improves Neurological Outcomes by Downregulating Hippocampal Autophagy and Apoptosis in an Asphyxia-Induced Cardiac Arrest and Resuscitation Rat Model

Chih-Hung Wang , MD, PhD; Chien-Hua Huang , MD, PhD; Min-Shan Tsai , MD, PhD; Chan-Chi Wang , MSc; Wei-Tien Chang, MD, PhD,* Shing-Hwa Liu , PhD; Wen-Jone Chen , MD, PhD*

BACKGROUND: Protracted cerebral hypoperfusion following cardiac arrest (CA) may cause poor neurological recovery. We hypothesized that inhaled carbon dioxide (CO₂) could augment cerebral blood flow (CBF) and improve post-CA neurological outcomes.

METHODS AND RESULTS: After 6-minute asphyxia-induced CA and resuscitation, Wistar rats were randomly allocated to 4 groups (n=25/group) and administered with different inhaled CO₂ concentrations, including control (0% CO₂), 4% CO₂, 8% CO₂, and 12% CO₂. Invasive monitoring was maintained for 120 minutes, and neurological outcomes were evaluated with neurological function score at 24 hours post-CA. After the 120-minute experiment, CBF was 242.3% (median; interquartile range, 221.1%–267.4%) of baseline in the 12% CO₂ group while CBF fell to 45.8% (interquartile range, 41.2%–58.1%) of baseline in the control group ($P<0.001$). CBF increased along with increasing inhaled CO₂ concentrations with significant linear trends ($P<0.001$). At 24 hours post-CA, compared with the control group (neurological function score, 9 [interquartile range, 8–9]), neurological recovery was significantly better in the 12% CO₂ group (neurological function score, 10 [interquartile range, 9.8–10]) ($P<0.001$) while no survival difference was observed. Brain tissue malondialdehyde ($P=0.02$) and serum neuron-specific enolase ($P=0.002$) and S100 β levels ($P=0.002$) were significantly lower in the 12% CO₂ group. TUNEL (terminal deoxynucleotidyl transferase–mediated biotin–deoxyuridine triphosphate nick-end labeling)-positive cell densities in hippocampal CA1 ($P<0.001$) and CA3 ($P<0.001$) regions were also significantly reduced in the 12% CO₂ group. Western blotting showed that beclin-1 ($P=0.02$), p62 ($P=0.02$), and LAMP2 (lysosome-associated membrane protein 2) ($P=0.01$) expression levels, and the LC3B-II:LC3B-I ratio ($P=0.02$) were significantly lower in the 12% CO₂ group.

CONCLUSIONS: Administering inhaled CO₂ augmented post-CA CBF, mitigated oxidative brain injuries, ameliorated neuronal injury, and downregulated apoptosis and autophagy, thereby improving neurological outcomes.

Key Words: apoptosis ■ autophagy ■ carbon dioxide ■ cardiac arrest ■ cerebral blood flow

Globally, out-of-hospital cardiac arrest (CA) affects an estimated 44 individuals per 100 000 on an annual basis.¹ The prognosis following this condition

is dismal, with only ~45% of patients² recovering neurological function after return of spontaneous circulation (ROSC).

Correspondence to: Wei-Tien Chang, MD, PhD, and Wen-Jone Chen, MD, PhD, No.7, Zhongshan S. Rd., Zhongzheng Dist., Taipei City 100, Taiwan (R.O.C.). Email: wchang@ntu.edu.tw; wjchen1955@ntu.edu.tw

* W.-T. Chang and W.-J. Chen contributed equally.

Supplemental Material is available at <https://www.ahajournals.org/doi/suppl/10.1161/JAHA.122.027685>

For Sources of Funding and Disclosures, see page 12.

© 2022 The Authors. Published on behalf of the American Heart Association, Inc., by Wiley. This is an open access article under the terms of the [Creative Commons Attribution-NonCommercial-NoDerivs](https://creativecommons.org/licenses/by-nc-nd/4.0/) License, which permits use and distribution in any medium, provided the original work is properly cited, the use is non-commercial and no modifications or adaptations are made.

JAHA is available at: www.ahajournals.org/journal/jaha

CLINICAL PERSPECTIVE

What Is New?

- Inhaled CO₂ could improve post-cardiac arrest neurological outcomes by augmenting cerebral blood flow.
- The mechanisms underlying the improvement of neurological outcomes by inhaled CO₂ involve both apoptosis and autophagy pathways.

What Are the Clinical Implications?

- Cerebral blood flow is a crucial determinant in post-cardiac arrest neurological recovery.
- Instead of adjusting ventilator settings to achieve desired pressure of arterial CO₂ level, inhaled CO₂ might be more applicable for patients with post-cardiac arrest to facilitate neurological recovery.

Nonstandard Abbreviations and Acronyms

CA	cardiac arrest
CBF	cerebral blood flow
EtCO₂	end-tidal CO ₂
iCO₂	inhaled CO ₂
NFS	neurological function scores
NSE	neuron-specific enolase
PaCO₂	pressure of arterial CO ₂
PbtO₂	partial pressure of brain tissue oxygenation
ROS	reactive oxygen species
ROSC	return of spontaneous circulation

Brain injury is a major component of post-CA syndrome,³ contributing to 65.2% of deaths during post-CA intensive care.⁴ Post-CA brain injury⁵ is caused by a primary injury (ie, the immediate cessation of cerebral oxygen delivery during CA), and secondary injuries after ROSC, including protracted cerebral hypoperfusion (ie, the so-called “no-reflow” phenomenon).^{6–8}

Cerebral oxygen delivery is determined by cerebral blood flow (CBF) and blood oxygen levels. A major determinant of CBF is partial pressure of arterial CO₂ (PaCO₂). Mild hypercapnia (end-tidal CO₂ [EtCO₂]: 45–50 mmHg) was reported to be associated with less neuronal degeneration in a porcine post-CA model.⁹ The administration of inhaled CO₂ (iCO₂) showed neuroprotective effects in cerebral ischemia-reperfusion injury rat models.^{10,11}

In this study, we hypothesized that iCO₂ may facilitate neurological recovery by augmenting CBF in rats

resuscitated from asphyxia-induced CA. We first monitored changes in CBF corresponding to different iCO₂ concentrations. Then, we compared clinical outcomes between different iCO₂ concentration groups. Finally, we examined the potential mechanisms underlying the neuroprotective effects of iCO₂, including mitochondrial biomarkers alterations, apoptosis, and autophagy mechanisms.¹²

METHODS

This research was approved by the Institutional Animal Care and Use Committee of College of Medicine, National Taiwan University (approval number 20180314), and was conducted according to Animal Research Reporting of In Vivo Experiments guidelines.¹³

Data Transparency and Openness

The data that support the findings of this study are available from the corresponding author upon reasonable request.

Animal Preparation

Animal studies were performed using an established asphyxia-induced CA and cardiopulmonary resuscitation (CPR) rat model.^{8,14} Briefly, 14-week-old male Wistar rats were anesthetized using intraperitoneal pentobarbital (45 mg/kg). Then, tracheal intubation with mechanical ventilation was initiated at a tidal volume of 0.6 mL/100 g body weight, a frequency of 100 breaths/min, and an inspired O₂ fraction of 21%. CBF and partial pressure of brain tissue oxygenation (PbtO₂) levels were continuously monitored using OxyFlo Pro and OxyLite Pro (Oxford-Optronix, Oxford, UK) instruments, respectively, via a fiber sensor (NX-BF/OFT/E, Oxford-Optronix) inserted through a small cranial window over the left hemisphere. The insertion site was marked on the dura with the stereotaxic coordinate anteroposterior (–3.5 mm) and lateral (2.0 mm) from the bregma. The fiber sensor was inserted 2 mm from the dura into the dorsal hippocampal CA1 region.¹⁵ The right femoral artery was cannulated to monitor arterial blood pressure and the left jugular vein cannulated to collect blood samples and administer medication. Rectal temperature was maintained at 36.5 °C to 37.5 °C.

Asphyxia-Induced CA and CPR

CA was induced 5 minutes after surgical preparation (Figure 1) by clamping the endotracheal tube. CA was defined as mean arterial pressure (MAP) ≤20 mmHg. CPR was started at 6 minutes after asphyxia, with 1 intravenous epinephrine (0.002 mg/100 g) dose, 1 sodium bicarbonate (1 mEq/kg) dose, and manual

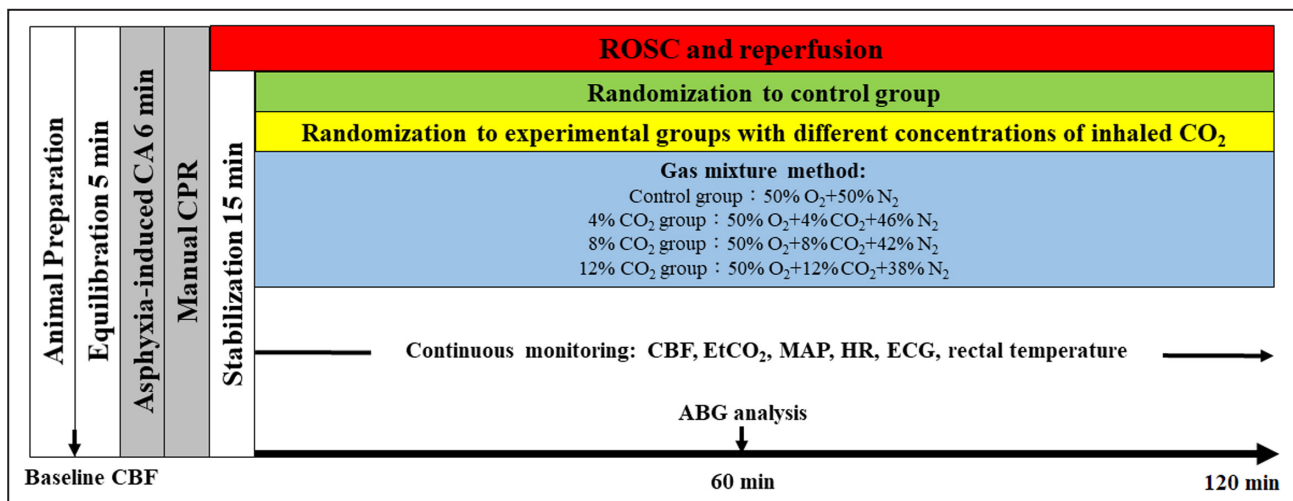


Figure 1. Study procedures and measurements at baseline, asphyxia, cardiac arrest and cardiopulmonary resuscitation, and reperfusion.

ABG indicates arterial blood gas; CA, cardiac arrest; CBF, cerebral blood flow; EtCO₂, partial pressure of end-tidal carbon dioxide; HR, heart rate; MAP, mean arterial pressure; and ROSC, return of spontaneous circulation.

chest compressions (200/min). During CPR, ventilatory inspired O₂ fraction was increased to 100%. The ROSC was defined as a MAP \geq 40mmHg for 10minutes. Rats were excluded if ROSC failed to occur within 10minutes of CPR.

Rats were randomly allocated to 4 study groups 15minutes after ROSC. Randomization was performed using a computer-generated random number list, with a block size of 4. Depending on group assignment, animals were ventilated at different iCO₂ concentrations for 105 minutes: 50% O₂+50% N₂ (control group), 50% O₂+4% CO₂+46% N₂ (4% CO₂ group), 50% O₂+8% CO₂+42% N₂ (8% CO₂ group), and 50% O₂+12% CO₂+38% N₂ (12% CO₂ group). EtCO₂ levels were continuously monitored (PhysioSuite, Kent Scientific Corporation, Torrington, CT) after ROSC. Point-of-care testing (Epic Blood Analysis System, Siemens Healthineers, Erlangen, Germany), including arterial blood analyses and concentrations of sodium, potassium, calcium, and creatinine, was conducted 60minutes post-ROSC. If necessary, intraperitoneal pentobarbital would be used for sedation after ROSC.

Outcome Measures of Survival and Neurological Recovery

After the 120-minute experiment, rats were returned to cages. At 24hours post-ROSC, rat survival status was recorded; neurological outcomes were assessed using rat neurological function scores (NFS) (Table S1)¹⁶ by researchers masked to treatment allocations. Rats were then humanely euthanized using intraperitoneal pentobarbital (45mg/kg). The brain tissues of 24-hour survival animals were harvested for Western blotting (WB), thiobarbituric acid reactive substance assay,

and TUNEL (terminal deoxynucleotidyl transferase-mediated biotin-deoxyuridine triphosphate nick-end labeling) assay. Right atrium blood samples were collected for ELISA and measuring concentrations of aspartate aminotransferase, alanine aminotransferase, and creatinine. Right hemispheres were washed in physiological saline, immediately frozen in liquid nitrogen, and stored at -80°C . Left hemispheres were immediately fixed in 4% formaldehyde in 0.1 M phosphate buffer.

Thiobarbituric Acid Reactive Substance Assay

The right hemispheres were homogenized in radioimmunoprecipitation assay buffer with protease and phosphatase inhibitors (#78441, Thermo Fisher Scientific, Waltham, MA). After centrifugation, the resulting supernatant was used for thiobarbituric acid reactive substance assay kit (#10009055, Cayman Chemical, Ann Arbor, MI) per manufacturer's instructions to measure concentrations of malondialdehyde, a product of lipid peroxidation caused by reactive oxygen species (ROS). Absorbance was measured on a microplate (SpectraMax Plus 384 Microplate reader, Molecular Devices, San Jose, CA).

ELISA Kits

ELISA kits of neuron-specific enolase (NSE) (#E-EL-R0058, Elabscience Biotechnology, Houston, TX), S100 β (#E-EL-R0868, Elabscience Biotechnology), and cardiac troponin I (#ab246529, Abcam, Cambridge, UK) were used to determine the injury biomarkers of brain and heart according to the

manufacturer's instructions. Absorbance was measured on a microplate (SpectraMax Plus 384 Microplate reader, Molecular Devices, San Jose, CA).

TUNEL Assay

Left hemispheres were assayed using the DeadEnd Fluorometric TUNEL System (Promega, Madison, WI) according to manufacturer's instructions. TUNEL assays were performed on 4- μ m paraffin-embedded sections. We used 4',6-diamidino-2-phenylindole to stain nuclei. Apoptotic cells were examined by confocal fluorescence microscopy (EVOS FL Auto Imaging System, Thermo Fisher Scientific, Waltham, MA). For each sample, viewing fields were randomly selected in hippocampal CA1 and CA3 regions for quantitative comparisons.¹⁷ Fields were photographed under microscopy at 510/542-nm (green TUNEL) and 447/460-nm wavelengths (bluish-violet 4',6-diamidino-2-phenylindole). PhotolImpact X3 (Corel, Ottawa, Canada) was used to merge images for final counting analyses in ImageJ software (Version 1.52a, National Institutes of Health, Bethesda, MD). TUNEL-positive cell densities in the aforementioned regions were measured at 50 \times magnification, with the area of each microscopic field \approx 0.48mm² (apoptotic cells/mm²).

Western Blotting

Right hemispheres were used for Western blotting. The primary antibodies, including Beclin-1 (#3738, Cell Signaling Technology, Danvers, MA), LC3B (#83506, Cell Signaling Technology), p62 (#39749, Cell Signaling Technology), LAMP2 (lysosome-associated membrane protein 2; #PA1-655, Invitrogen, Waltham, MA), caspase-3 (#14220, Cell Signaling Technology), PARP (#9542, Cell Signaling Technology), Bcl-2 (#GTX100064, GeneTex, Irvine, CA), Bax (#GTX109683, GeneTex), and cytochrome c (#GTX108585, GeneTex) were used. Beta-actin (HRP-60008, Proteintech Group, Rosemont, IL) was used as a loading control.

Statistical Analysis

We a priori planned to compare the primary outcome, NFS, between the 12% CO₂ group and the control group to observe the effects of iCO₂. Both 4% CO₂ and 8% CO₂ concentrations were used for exploratory analyses to investigate if iCO₂ effects could be achieved by lower iCO₂ concentrations and to also check for trends among study groups. Accordingly, 17 animals/group were required to demonstrate a mean difference of 1.5 in NFS, with a power of 80% at the 5% level, and an SD of 1.5 (MedCalc, version 20.011, MedCalc Software, Ostend, Belgium). From our previous studies,^{8,14} the 24-hour survival rate of post-ROSC

rats in the control group was \approx 70%; therefore, the sample size for each group was calculated at 25 to compensate for losses.

CBF was expressed as the proportion of the baseline (%baseline) and delta of PbtO₂ was computed by PbtO₂ at a certain time point minus the baseline.¹⁸ Categorical data were expressed as counts and proportions and compared using a Chi-squared test. Continuous data were expressed as median and interquartile range and compared using the Kruskal–Wallis test. A post hoc Dunn test was used for pairwise comparisons between each experimental group and the control group. Trend analysis was performed using Jonckheere–Terpstra test or Chi-squared test for trend. Time-based measurements were compared using 2-way repeated measurement ANOVA. Survival curves were determined with the Kaplan–Meier method and compared with the log-rank test. Between-group comparisons were made with all available data. For the NFS, a sensitivity analysis was performed to test whether the missing NFS in rats with early death would influence the results, including (1) best scenario: in each experimental group, the rats with early death would be assigned with the median NFS of the experimental rats surviving 24 hours while in the control group, the rats with early death would be assigned with an NFS of zero point; and (2) worst scenario: in the control group, the rats with early death would be assigned with the median NFS of the control rats surviving 24 hours while in the experimental groups, the rats with early death would be assigned with an NFS of zero point.

A 2-tailed $P < 0.05$ was considered statistically significant. All statistical tests were performed in GraphPad Prism Version 9.2.0 (GraphPad Software, La Jolla, CA) and IBM SPSS Statistics for Windows, version 28.0.1.1 (IBM Corp., Armonk, NY).

RESULTS

Baseline Characteristics and Resuscitation Variables

In total, 120 rats were used for experiments and 100 rats randomized to study groups (Figure S1). No significant differences were observed in baseline characteristics and resuscitation variables among groups (Table 1).

Physiological Parameters During Invasive Monitoring

As shown (Figure 2 and Table 1), in the control group, after the initial hyperemia state, CBF decreased gradually and fell to \approx 45.8% of baseline at 120 minutes post-ROSC. In contrast, CBF was increased gradually by iCO₂. In the 12% CO₂ group, CBF at 120 minutes post-ROSC was 242.3% of baseline, significantly higher

Table 1. Baseline Characteristics, Peri-Resuscitation Variables, and Outcomes of Randomized Animals

Variables	Control group (n=25)	4% CO ₂ group (n=25)	8% CO ₂ group (n=25)	12% CO ₂ group (n=25)	P value (Kruskal–Wallis test)	P value (Jonckheere–Terpstra test)
Baseline characteristics and resuscitation variables						
Body weight, g	450 (420–471)	460 (440–486)	445 (440–470)	456 (424–486)	0.56	0.60
Cardiac arrest time, s	162 (148–170)	159 (146–175)	161 (152–174)	161 (152–174)	0.90	0.83
CPR time, s	65 (55–235)	61 (56–106)	74 (44–337)	77 (58–161)	0.85	0.56
Point-of-care testing at 60-min post-ROSC						
pH	7.331 (7.314–7.360) (n=20)	7.239 (7.226–7.247) (n=21)	7.140 (7.130–7.151) (n=18)	7.067 (7.047–7.360) (n=21)	<0.001	<0.001
PaCO ₂ , mmHg	51.5 (50.5–54.7) (n=20)	72.5 (70.3–76.9) (n=21)	98.7 (93.8–103.1) (n=18)	121.3 (119.8–126.2) (n=21)	<0.001	<0.001
PaO ₂ , mmHg	233.4 (184.9–292.5) (n=20)	221.9 (208.9–253.5) (n=21)	231.8 (218.9–247.3) (n=18)	267.1 (228.7–284.3) (n=21)	0.09	0.05
HCO ₃ ⁻ , mEq/L	29.4 (27.0–30.6) (n=20)	32.2 (29.7–33.5) (n=21)	33.0 (32.1–34.5) (n=18)	35.4 (32.8–36.8) (n=21)	<0.001	<0.001
Lactate, mg/dL	7.3 (5.6–11.3) (n=20)	4.5 (3.1–6.5) (n=21)	2.7 (2.7–2.8) (n=18)	2.7 (2.7–4.8) (n=21)	<0.001	<0.001
Sodium, mEq/L	142.5 (141.0–143.8) (n=20)	143.0 (143.0–145.5) (n=21)	146.0 (142.8–147.0) (n=18)	146.0 (145.0–147.0) (n=21)	<0.001	<0.001
Potassium, mEq/L	3.8 (3.7–4.1) (n=20)	3.8 (3.6–3.9) (n=21)	3.8 (3.6–3.9) (n=18)	4.0 (3.6–4.4) (n=21)	0.60	0.98
Calcium, mg/dL	5.1 (5.0–5.3) (n=20)	5.2 (5.1–5.5) (n=21)	5.4 (5.3–5.5) (n=18)	5.4 (5.3–5.8) (n=21)	<0.001	<0.001
Creatinine, mg/dL	0.64 (0.50–0.67) (n=20)	0.71 (0.62–0.76) (n=21)	0.75 (0.62–0.82) (n=18)	0.74 (0.58–1.03) (n=21)	0.10	0.03
Physiological parameters at 120-min post-ROSC						
CBF level, % of baseline	45.8 (41.2–58.1) (n=20)	155.5 (134.0–175.1) (n=20)	192.4 (183.6–215.6) (n=18)	242.3 (221.1–267.4) (n=21)	<0.001	<0.001
ΔPbtO ₂ , mmHg	1.26 (-1.78–11.74) (n=20)	14.39 (0.20–25.44) (n=20)	22.22 (8.25–35.09) (n=18)	29.81 (12.57–55.60) (n=21)	0.001	<0.001
EtCO ₂ , mmHg	51 (47–54) (n=20)	77 (71–81) (n=20)	100 (97–104) (n=18)	127 (124–129) (n=21)	<0.001	<0.001
MAP, mmHg	110.4 (103.6–112.0) (n=20)	116.9 (102.5–129.9) (n=20)	114.9 (102.0–117.7) (n=18)	109.2 (100.1–117.2) (n=21)	0.53	0.62
Brain injury biomarkers at 24-h post-ROSC						
NSE level at 24 h, ng/mL	0.552 (0.483–0.732) (n=10)	0.369 (0.316–0.454) (n=10)	0.419 (0.394–0.520) (n=9)	0.374 (0.364–0.443) (n=10)	0.001	0.02
S100β level, pg/mL	1.706 (1.612–1.868) (n=10)	1.420 (1.384–1.436) (n=10)	1.432 (1.409–1.500) (n=9)	1.414 (1.392–1.472) (n=10)	0.04	0.05
Malondialdehyde level, μM	49.15 (47.24–49.84) (n=5)	43.26 (42.69–46.68) (n=5)	44.67 (44.04–46.98) (n=5)	43.35 (42.65–44.05) (n=5)	0.03	0.03
Cardiac, renal, and hepatic biomarkers at 24 h post-ROSC						
Cardiac troponin I, pg/mL	0.238 (0.139–0.423) (n=20)	0.057 (0.031–0.210) (n=20)	0.214 (0.109–0.420) (n=18)	0.107 (0.062–0.166) (n=21)	<0.001	0.24
AST, U/L	915.5 (248.6–2036.0) (n=20)	557.7 (157.6–848.0) (n=20)	764.3 (400.9–1398.0) (n=18)	576.3 (459.3–838.5) (n=21)	0.26	0.15
ALT, U/L	162.5 (33.8–297.8) (n=20)	85.5 (43.0–167.5) (n=20)	128.5 (54.5–222.3) (n=18)	98.0 (75.5–145.5) (n=21)	0.45	0.33
Creatinine, mg/dL	0.30 (0.20–0.30) (n=20)	0.25 (0.20–0.30) (n=20)	0.30 (0.18–0.33) (n=18)	0.30 (0.20–0.30) (n=21)	0.92	0.86
Outcomes at 24 h post-ROSC						
Survival, n (%)	20 (80)	20 (80)	18 (72)	21 (84)	0.77 [†]	0.82 [†]
Neurological function score	9 (8–9) (n=20)	9 (8–9) (n=20)	10 (9–10) (n=18)	10 (9.8–10) (n=21)	<0.001	<0.001

Data are expressed as the median (interquartile range) or counts (proportions). ALT indicates alanine aminotransferase; AST, aspartate aminotransferase; CBF, cerebral blood flow; CPR, cardiopulmonary resuscitation; ΔPbtO₂, delta of partial pressure of brain tissue oxygenation; EtCO₂, partial pressure of end-tidal carbon dioxide; HCO₃⁻, sodium bicarbonate; MAP, mean arterial pressure; NSE, neuron-specific enolase; PaCO₂, arterial partial pressure of carbon dioxide; PaO₂, arterial partial pressure of oxygen; ROSC, return of spontaneous circulation; and NA, not available. The results of post hoc pairwise comparisons were annotated in corresponding figures.

[†]This comparison was performed using the Chi-squared test.

^{††}This comparison was performed using the Cochran–Armitage test for trend.

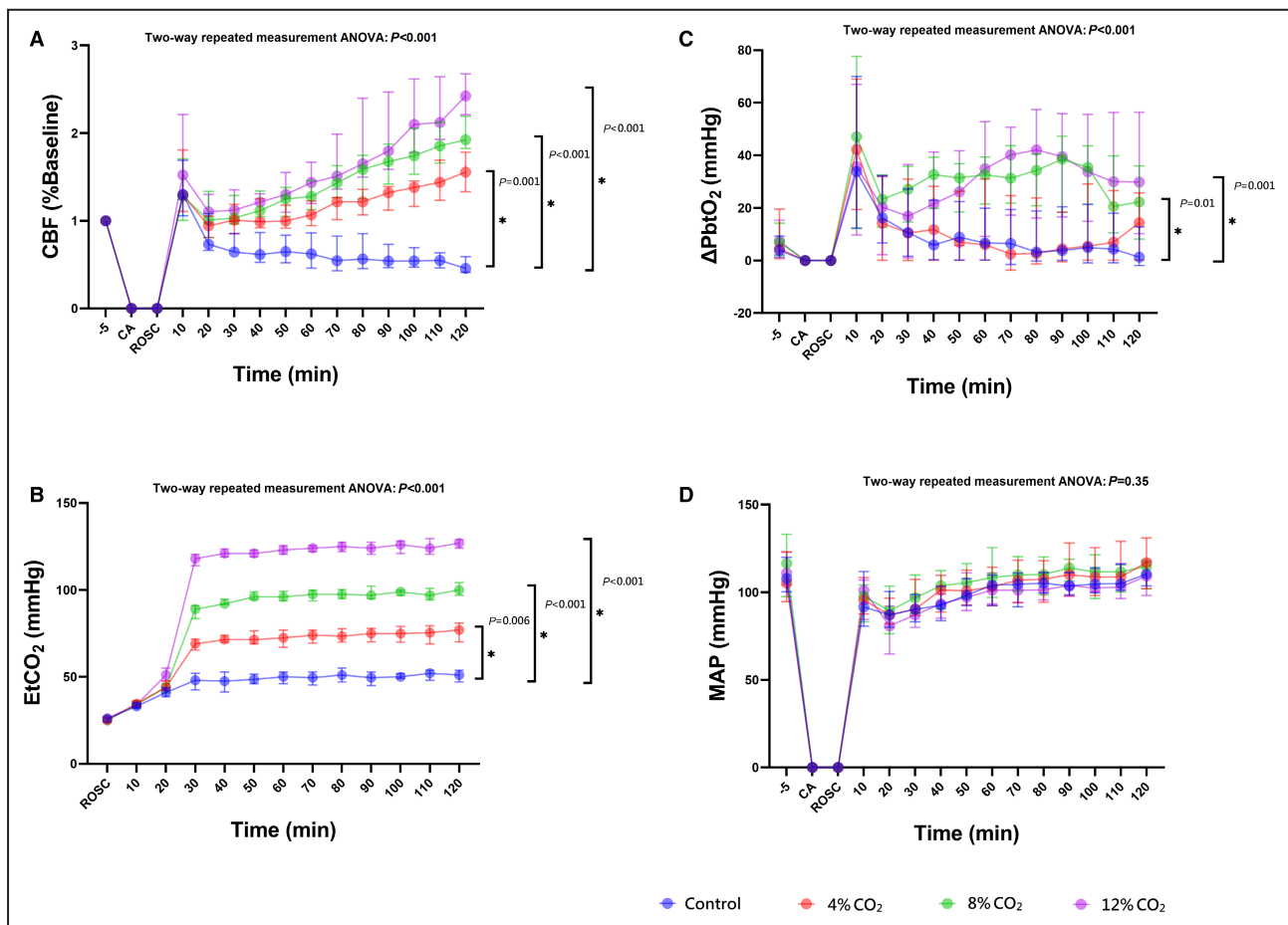


Figure 2. Physiological parameters during invasive monitoring.

The administration of inhaled CO₂ increased cerebral blood flow, end-tidal CO₂, partial pressure of brain tissue oxygenation without compromising mean arterial pressure. Data are presented as the median and interquartile range. Pairwise comparisons of physiological parameters at 120 minutes post-return of spontaneous circulation between experimental and control groups were performed by the post hoc Dunn test. The asterisk indicates statistical significance. CA indicates cardiac arrest; CBF, cerebral blood flow; ΔPbtO₂, delta of partial pressure of brain tissue oxygenation; EtCO₂, partial pressure of end-tidal carbon dioxide; iCO₂, inhaled carbon dioxide; MAP, mean arterial pressure; and ROSC, return of spontaneous circulation.

than the control group. A significant increasing trend was also observed in CBF levels with increasing iCO₂ concentrations. EtCO₂ levels plateaued at 30 minutes post-ROSC after an initial rapid increase. At 60 minutes post-ROSC, significant differences in PaCO₂ were noted among experimental groups. At 120 minutes post-ROSC, ΔPbtO₂ levels were significantly higher in 12% CO₂ animals than controls. MAP levels were not significantly different among groups.

Survival and Neurological Outcomes

No significant differences in 24-hour survival rates were observed among groups (Table 1, Figure S2). There was significant difference in cardiac troponin I (Table 1); compared with the control group, the cardiac troponin I level was significantly lower in the 12% CO₂ group (P=0.003). For rats surviving to 24 hours, NFS were significantly higher in the 12% CO₂ group when

compared with control animals (Figure 3A). The sensitivity analysis revealed that the 12% CO₂ group still demonstrated higher NFS than the control group after accounting for the rats with early death (Figure S3).

Oxidative and Neuronal Injuries

Brain tissue malondialdehyde and serum NSE and S100β levels were consistently lower in the 12% CO₂ group when compared with control animals (Figure 3B through 3D, Table 1), suggesting less oxidative and neuronal injuries in the former group.

Apoptosis Downregulation

TUNEL assay data revealed significantly lower apoptotic cell densities in the hippocampal CA1 and CA3 regions of the 12% CO₂ group when compared with controls (Figure 4A through 4C). Nonetheless, no significant differences were observed in expression of

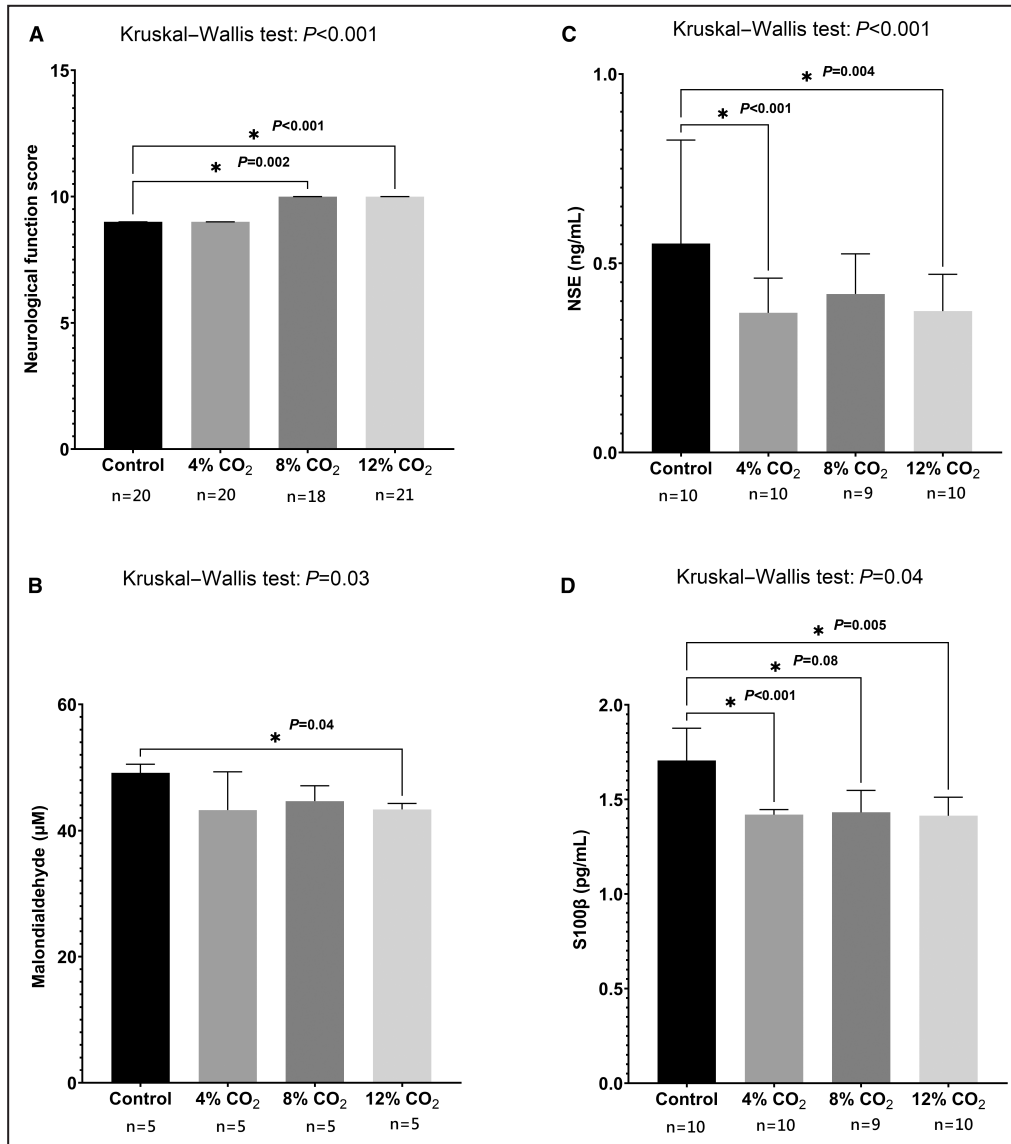


Figure 3. Neurological outcomes and brain injury biomarkers at 24 hours post-return of spontaneous circulation.

Compared with the control group, the neurological function score was higher in the 12% CO₂ group, suggesting better neurological recovery. The oxidative injuries, as indicated by the brain tissue malondialdehyde level, were lower in the 12% CO₂ group. Also, the neuronal injuries, as represented by the serum neuron-specific enolase and S100β concentrations, were lower in the 12% CO₂ group. Data are presented as the median and third quartile. Pairwise comparisons of neurological outcomes or biomarker levels between experimental and control groups were performed using the post hoc Dunn test. Samples were randomly selected for measuring malondialdehyde, neuron-specific enolase, and S100β levels. The asterisk indicates statistical significance. NSE indicates neuron-specific enolase.

mitochondrial biomarkers, caspase-3 activation, or PARP cleavage (Figure 5).

Autophagy Downregulation

As shown (Figure 6), beclin-1 and LAMP2 expression levels, and the LC3B-II:LC3B-I ratio were consistently lower in the 12% CO₂ group when compared with controls, suggesting autophagy was downregulated in the former group.

DISCUSSION

Main Findings

Firstly, we observed that increasing iCO₂ concentrations would result in increasing CBF. Secondly, when compared with control animals, the 12% CO₂ group showed better neurological recovery. Thirdly, the neuroprotective effects induced by iCO₂ could be explained by mitigated ROS production, less

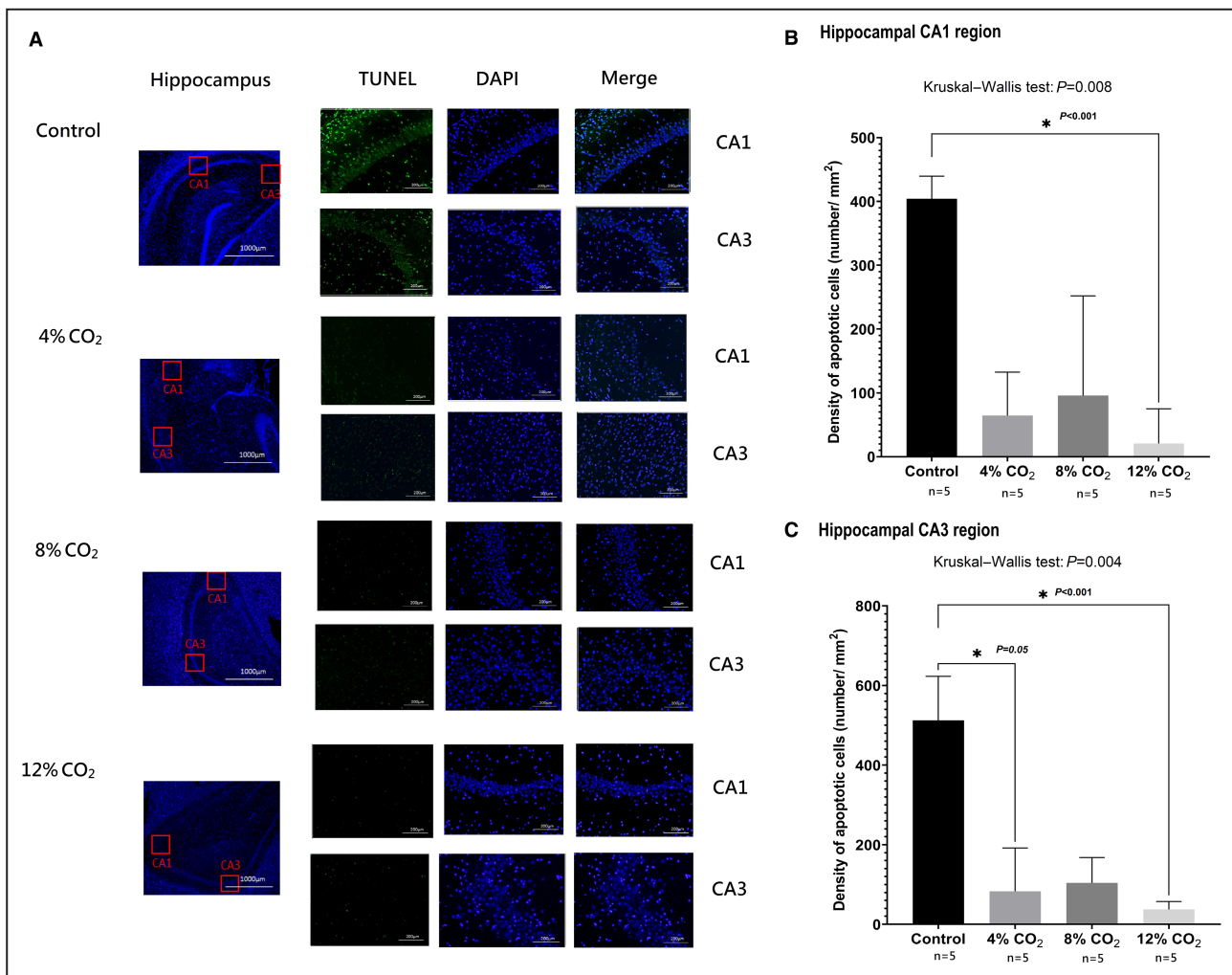


Figure 4. TUNEL staining in hippocampus.

The lower hippocampal TUNEL-positive cell densities suggest reduced apoptotic cells in the 12% CO₂ group than the control group. Data are presented as the median and third quartile. Pairwise comparisons between experimental and control groups were performed by the post hoc Dunn test. Samples were randomly selected for TUNEL stain. **A**, Brain sections were stained for TUNEL (green) and 4',6-diamidino-2-phenylindole (bluish-violet). Confocal microscopy was used to image hippocampal CA1 and CA3 regions at 50× magnification. Red rectangles indicate selected CA1 and CA3 regions for quantification. The scale bar represents 200 μm. **B** and **C**, Apoptotic cell densities in CA1 and CA3 regions. The asterisk indicates statistical significance. DAPI indicates 4',6-diamidino-2-phenylindole; and TUNEL, terminal deoxynucleotidyl transferase–mediated biotin–deoxyuridine triphosphate nick-end labeling.

neuronal injury, and downregulated apoptosis and autophagy.

Augmented Post-CA CBF Levels and Improved Neurological Outcomes

Previous studies^{10,11} demonstrated that iCO₂ was neuroprotective for cerebral ischemia-reperfusion injury; nonetheless, the changes in CBF were not demonstrated. Because vascular reactivity to CO₂ may be attenuated in the early post-CA period,¹⁹ the neuroprotective effects of iCO₂ may not be directly attributed to augmented CBF if CBF is not monitored. As shown in the control group (Figure 2A), after initial hyperemia peaked at ~10 minutes post-ROSC, CBF

levels continued decreasing until the end of observations, revealing the so-called “no-reflow” phenomenon.^{20,21} In contrast, when iCO₂ was administered, CBF levels began to rise 20 minutes post-ROSC. Even when EtCO₂ had plateaued at 30 minutes post-ROSC (Figure 2B), CBF levels were still rising. These data supported our hypothesis that iCO₂ exerted neuroprotective effects as it improved post-CA CBF during the no-reflow period.

Furthermore, trend analyses indicated a putative linear relationship between iCO₂ concentrations and CBF changes (Table 1). However, when compared with the control group, only the 12% CO₂ group showed consistently better results across all outcomes. Because sample sizes were estimated

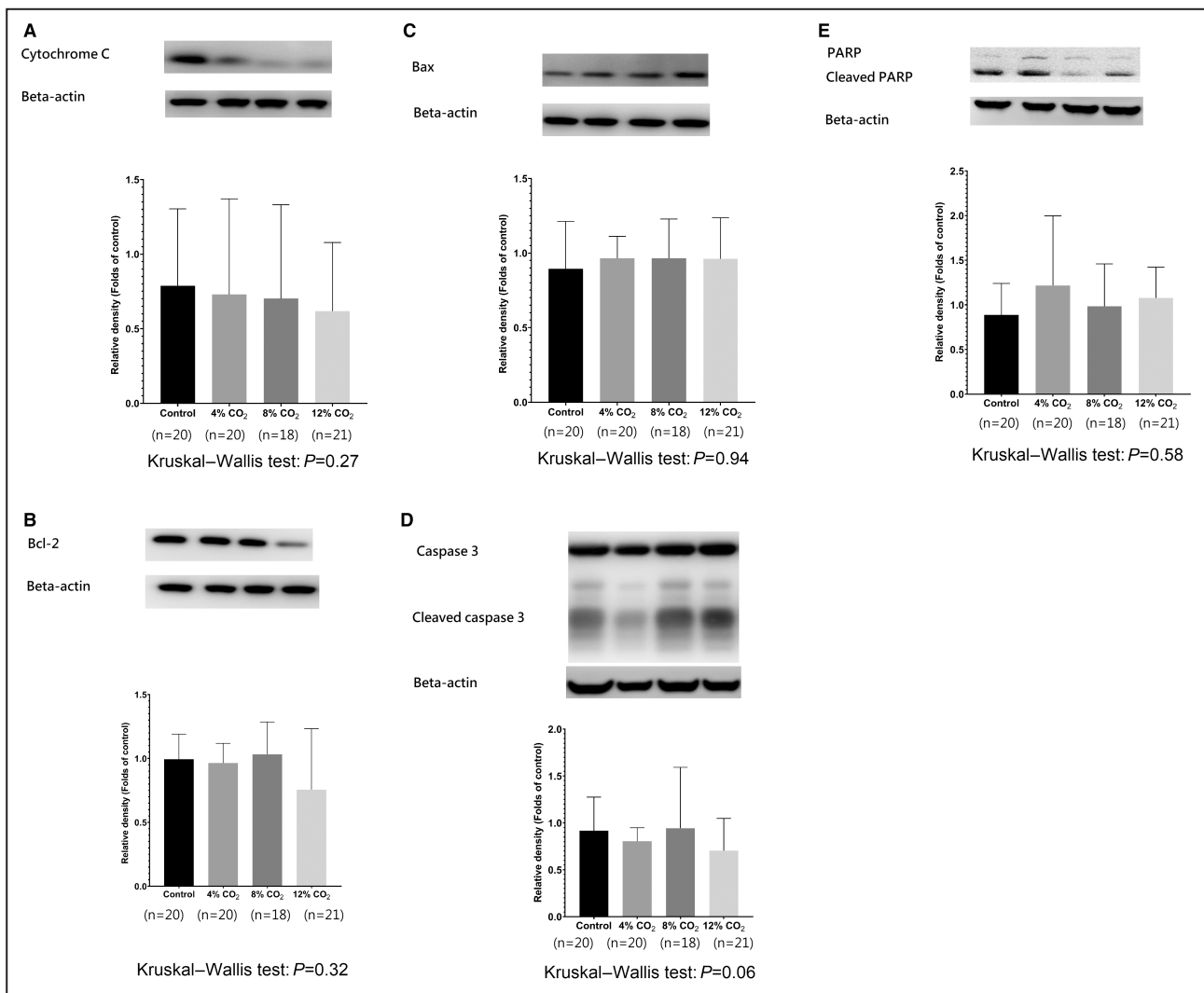


Figure 5. Western blotting of brain tissues.

Reactive oxygen species may activate the mitochondrial pathway leading to execution of apoptosis. Compared with the control group, no difference in the expression of cytochrome c, Bcl-2, or Bax was observed. Caspase-3 activation and PARP cleavage served as a proxy of execution of apoptosis pathway; also, no significant between-group differences are noted. Data are presented as the median and third quartile. **A through C**, Comparisons of expression level of cytochrome c, Bcl-2, and Bax in brain tissue by Western blotting. **D and E**, Comparisons of ratios between full-length and cleaved caspase 3 or PARP in brain tissue by Western blotting.

by assumed differences in NFS between the control and the 12% CO₂ group, our sample size may have been insufficient to show significant differences between the control and the 4% CO₂ or 8% CO₂ groups. Nevertheless, in terms of all outcomes, significant linear trends were identified for improved neuroprotective effects with increasing iCO₂ concentrations, suggesting iCO₂ was generally beneficial for post-CA neurological recovery, rather than being only effective at concentrations of 12%.

Interestingly, 24-hour survival rates were not significantly different among study groups despite significant between-group differences in blood pH (Table 1). Acidosis was suggested to exert adverse effects on heart contractility^{22,23} and was associated with worse

clinical outcomes after ROSC.²⁴ However, MAP was not significantly different among study groups (Figure 2D). Furthermore, lactate levels were significantly lower with increasing iCO₂ concentration (Table 1). Previous studies reported that hypercapnic acidosis suppressed systemic lactate production during systemic hypoxemia²⁵ and was protective toward myocardial ischemia.²⁶ Furthermore, lower levels of aspartate transaminase and alanine transaminase were also noted in the groups administered with iCO₂. Despite that the between-group differences in both liver injury markers were not statistically different (Table 1), it was possible that iCO₂ facilitated the liver recovery process after ischemia-reperfusion injuries,²⁷ thereby expediting lactate clearance.

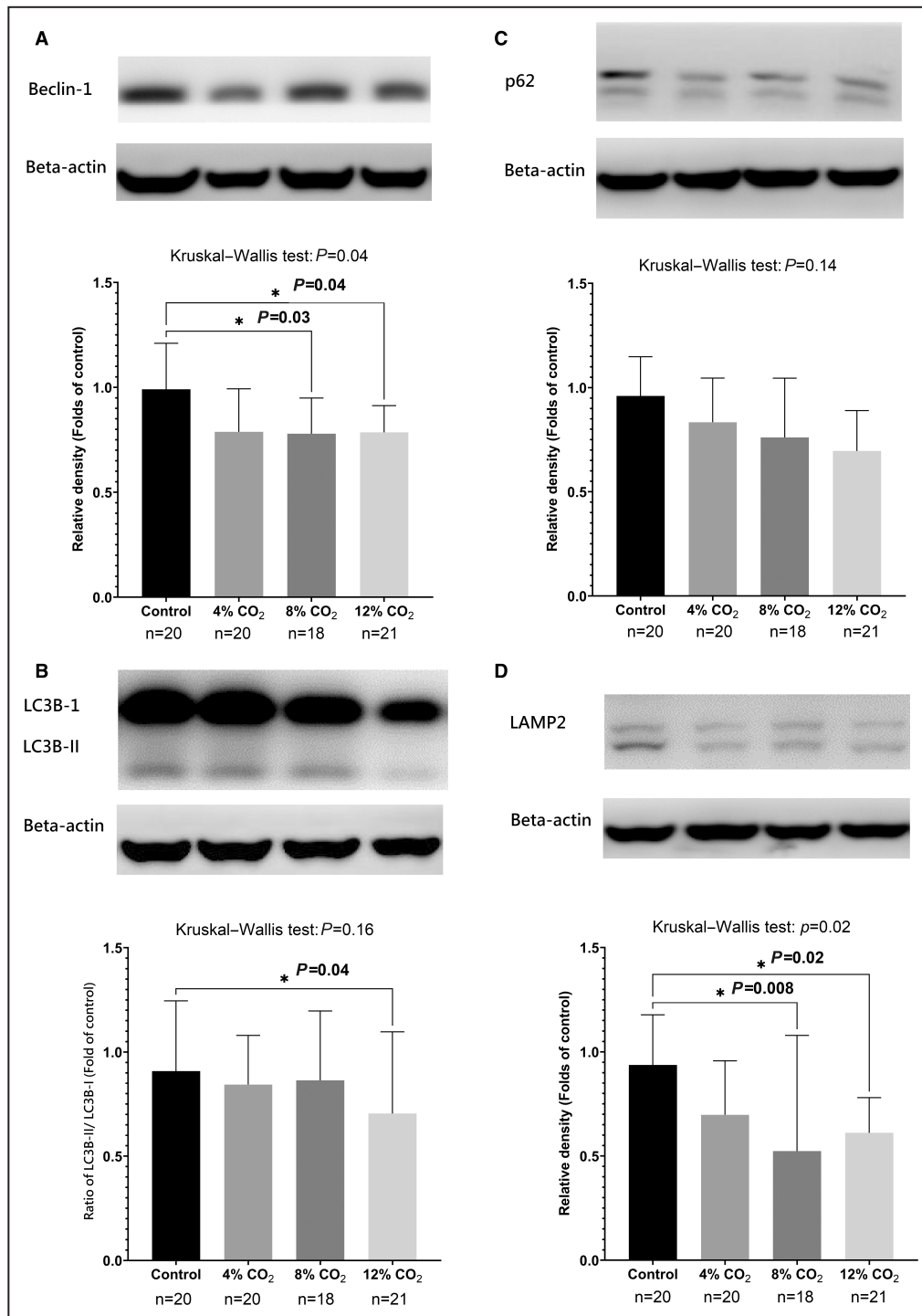


Figure 6. Western blot analysis of beclin-1, LC3B, p62, and LAMP2 expression.

Reduced expression levels of beclin-1 and LAMP2 and lower LC3B-II:LC3B-I suggest downregulation of autophagy. Data are presented as the median and third quartile. Pairwise comparisons of protein expression levels or ratios between experimental and control groups were performed using the post hoc Dunn test. The asterisk indicates statistical significance. LAMP2 indicates lysosome-associated membrane protein 2.

Thus, by improving post-CA no-reflow phenomenon, iCO₂ facilitated neurological recovery without significantly compromising hemodynamics and survival.

Attenuated Oxidative and Neuronal Injuries

Abrupt cessation of cerebral oxygen delivery caused primary post-CA brain injury.⁵ Cerebral oxygen delivery

could be adjusted by manipulating CBF or blood oxygen levels. Ventilating patients with high oxygen levels is a frequently used method to increase blood oxygen and increase oxygen delivery to the brain. However, resulting hyperoxia was associated with poor post-CA neurological recovery,^{28,29} which may have been attributed partly to increased ROS production and associated oxidative injuries.^{30,31} In our study, iCO₂ augmented CBF, thereby increasing cerebral oxygen delivery and PbtO₂. This result was consistent with the pilot trial conducted by Jakkula et al,³² which demonstrated higher near-infrared spectroscopy-measured regional cerebral oxygen saturation in patients with PaCO₂ targeted at 44 to 46 mmHg than those with PaCO₂ targeted at 33 to 35 mmHg. Cerebral reoxygenation reduced ROS-associated oxidative injuries, as indicated by lower malondialdehyde levels, and neuronal injuries as indicated by lower NSE and S100β levels (Figure 3).³³ In contrast to administering high oxygen levels, administering iCO₂ appeared to be a safer method to reoxygenate the brain effectively after asphyxia-induced CA.

Downregulating Apoptosis and Autophagy

We showed that iCO₂ mitigated neuronal apoptosis, as evidenced by reduced TUNEL-positive cell densities in hippocampal CA1 and CA3 regions (Figure 4). ROS may activate the mitochondrial pathways, leading to the release of cytochrome c and execution of apoptosis.³⁴ Therefore, reduced ROS levels in the 12% CO₂ group may have partly accounted for the attenuated apoptosis seen in these animals. Apoptosis is mainly executed by caspase-3, whereas PARP, a DNA repair enzyme, is selectively cleaved by activated caspase-3 during apoptosis.^{35–37} Therefore, caspase-3 activation and PARP cleavage have been viewed as hallmark apoptosis indicators. Interestingly, we detected no significant differences in caspase-3 activation or PARP cleavage among groups (Figure 4), which may be explained by several reasons. Firstly, we used the whole hemisphere rather than specifically the hippocampus to investigate apoptotic pathways. Because TUNEL-positive cells were most densely distributed in the hippocampus, containing other brain regions in Western blot analysis may dilute the differences. Secondly, Western blot analysis was performed using brain tissue harvested at 24 hours post-CA. At this time, initial apoptosis phases may have been completed.

It was reported that after ROSC, autophagy was initially activated, followed by apoptosis, and culminated in hippocampal neuronal death.¹² Autophagy (or macroautophagy) is an orchestrated cell catabolic process that eliminates damaged cytoplasmic contents³⁸ during various stress conditions (eg, hypoxia, nutrient starvation, and oxidative stress). During the process,³⁹

beclin-1 initiates autophagosome formation, LC3B elongates the autophagosome, and LAMP2 is required for autophagolysosome formation. During elongation, LC3B is first cleaved to LC3B-I and then converted to LC3B-II. Thus, the LC3B-II:LC3B-I ratio is used to monitor autophagy flux. We showed that beclin-1 and LAMP2 expression levels and the LC3B-II:LC3B-I ratio were reduced in the 12% CO₂ group, suggesting iCO₂ putatively downregulated autophagy (Figure 6). In contrast, p62 is a scaffold for protein aggregates destined for autophagolysosome degradation and should have accumulated when autophagy was downregulated. Nonetheless, our study did not identify significant difference in p62 level between the 12% CO₂ and control groups (Figure 6). It was possible that p62 may interact with multiple pathways other than autophagy and, therefore, it could be a less specific indicator for autophagy flux.⁴⁰ It should be emphasized that the changes in these autophagy markers may only be viewed as indirect evidence of the iCO₂ effects. Using autophagy inducer, such as rapamycin, or autophagy inhibitor, such as SP600125, to study the autophagic flux may be a better way to delineate the changes in autophagic flux caused by iCO₂ and may be considered in future studies, for which our study results may serve as the basis to select the optimal iCO₂ concentration for investigation.

Taken together, these results suggest that when post-CA CBF is augmented by iCO₂, neuronal stress is ameliorated, and autophagy might revert to a basal state to function as a potential prosurvival mechanism, concomitant with downregulated apoptosis.⁴¹

Future Directions

To date, the clinical evidence on post-CA PaCO₂ effects toward neurological outcomes is inconsistent.⁴² In 2 small randomized-controlled pilot trials, Eastwood et al⁴³ reported that PaCO₂ at 50 to 55 mmHg attenuated NSE release when compared with PaCO₂ at 35 to 45 mmHg, while Jakkula et al showed no difference in release of NSE³² and neurofilament light⁴⁴ between PaCO₂ at 44 to 46 mmHg and PaCO₂ at 33 to 35 mmHg. The latest 2020 American Heart Association⁴⁵ and 2021 European Resuscitation Council/ European Society of Intensive Care Medicine guidelines⁴⁶ recommended that post-CA PaCO₂ should be maintained within the normal physiological range, 35 to 45 mmHg. Our study demonstrated that increasing PaCO₂ levels were associated with better neuroprotective effects (Table 1). Nonetheless, in a rat model of transient global cerebral ischemia-reperfusion injury, Zhou et al¹⁰ noted PaCO₂ between 100 and 120 mmHg increased brain injury, which may be caused by increased brain edema. Therefore, further research is warranted to investigate the safety and neuroprotective effects of targeting higher PaCO₂ levels for patients

with post-CA. On the other hand, targeting personalized PaCO₂ levels by monitoring cerebral tissue oxygenation may also be an alternative to balancing risk and safety of iCO₂.

Study Limitations

First, we only assessed short-term neurological outcomes without performing neurobehavioral tests to evaluate long-term cognitive injuries. Second, we used inspired O₂ fraction of 50% during the initial post-ROSC period, resulting in elevated PaO₂ levels higher than recommended by guidelines.^{45,46} Future studies should further investigate whether the neuroprotective effects of iCO₂ would be influenced by different PaO₂ levels. Third, we used asphyxia-induced CA model to study the protective effects of iCO₂. However, in adult patients, the most prevalent cause of collapse was ventricular fibrillation or pulseless ventricular tachycardia, constituting 24% to 35% of out-of-hospital CA events.¹ In a rat study, Drabek et al⁶ noted that both ventricular fibrillation- and asphyxia-induced CA resulted in delayed hypoperfusion in all regions, including hippocampus. Because the delayed hypoperfusion phenomenon was common in both models, the benefits of iCO₂ observed in our asphyxia-induced CA model may still exist in ventricular fibrillation-induced CA model, which deserved further experiments and clinical studies. Fourth, according to the trend analysis, iCO₂ concentration <12% might be effective for post-ROSC brain injuries in general. Nonetheless, our study results may not be externally generalized to iCO₂ concentration >12% because some adverse effects of severe hypercapnia had been observed in different brain injury models.¹⁰ Finally, the ability to tolerate hypercapnic acidosis may be different between rats and human subjects. Before its application in clinical trials, more studies are needed to explore the safety of iCO₂ in patients with fragile post-ROSC.

CONCLUSIONS

Administering iCO₂ could increase post-CA CBF and facilitate neurological recovery. The neuroprotective effects of iCO₂ could be attributable to mitigated oxidative injury, reduced neuronal injury, and downregulated apoptosis and autophagy. Further research is required to examine the safety and neuroprotective effects of iCO₂ in clinical settings.

ARTICLE INFORMATION

Received August 1, 2022; accepted September 19, 2022.

Affiliations

Department of Emergency Medicine, National Taiwan University Hospital, Taipei, Taiwan (C.W., C.H., M.T., C.W., W.C., W.C.); Department of Emergency Medicine, College of Medicine (C.W., C.H., M.T., C.W., W.C., W.C.); and Institute of Toxicology, College of Medicine (S.L.), National Taiwan University,

Taipei, Taiwan; Department of Medical Research, China Medical University Hospital, China Medical University, Taichung, Taiwan (S.L.); Department of Pediatrics, National Taiwan University Hospital, Taipei, Taiwan (S.L.); Division of Cardiology, Department of Internal Medicine, National Taiwan University Hospital and National Taiwan University College of Medicine, Taipei, Taiwan (W.C.); and Division of Cardiology, Department of Internal Medicine, Min-Shen General Hospital, Taoyuan, Taiwan (W.C.).

Acknowledgments

We thank the staff of the 3rd Core Lab, Department of Medical Research, National Taiwan University Hospital, for technical support. We thank Dr Chih-Fan Yeh at Department of Internal Medicine, National Taiwan University Hospital, Taipei, for statistical support.

Sources of Funding

Dr Chih-Hung Wang received a grant (108-2628-B-002-016-, 109-2628-B-002-045-, 110-2628-B-002-028-) from the Ministry of Science and Technology. Ministry of Science and Technology had no involvement in designing the study, collecting, analyzing or interpreting the data, writing the manuscript, or deciding whether to submit the manuscript for publication.

Disclosures

None.

Supplemental Material

Table S1
Figures S1–S3

REFERENCES

- Berdowski J, Berg RA, Tijssen JG, Koster RW. Global incidences of out-of-hospital cardiac arrest and survival rates: systematic review of 67 prospective studies. *Resuscitation*. 2010;81:1479–1487. doi: [10.1016/j.resuscitation.2010.08.006](https://doi.org/10.1016/j.resuscitation.2010.08.006)
- Dankiewicz J, Cronberg T, Lilja G, Jakobsen JC, Levin H, Ullén S, Rylander C, Wise MP, Oddo M, Cariou A, et al. Hypothermia versus normothermia after out-of-hospital cardiac arrest. *N Engl J Med*. 2021;384:2283–2294. doi: [10.1056/NEJMoa2100591](https://doi.org/10.1056/NEJMoa2100591)
- Nolan JP, Neumar RW, Adrie C, Aibiki M, Berg RA, Bottiger BW, Callaway C, Clark RS, Geocadin RG, Jauch EC, et al. Post-cardiac arrest syndrome: epidemiology, pathophysiology, treatment, and prognostication. A Scientific Statement from the International Liaison Committee on Resuscitation; the American Heart Association Emergency Cardiovascular Care Committee; the Council on Cardiovascular Surgery and Anesthesia; the Council on Cardiopulmonary, Perioperative, and Critical Care; the Council on Clinical Cardiology; the Council on Stroke. *Resuscitation*. 2008;79:350–379. doi: [10.1016/j.resuscitation.2008.09.017](https://doi.org/10.1016/j.resuscitation.2008.09.017)
- Lemiale V, Dumas F, Mongardon N, Giovanetti O, Charpentier J, Chiche JD, Carli P, Mira JP, Nolan J, Cariou A. Intensive care unit mortality after cardiac arrest: the relative contribution of shock and brain injury in a large cohort. *Intensive Care Med*. 2013;39:1972–1980. doi: [10.1007/s00134-013-3043-4](https://doi.org/10.1007/s00134-013-3043-4)
- Sekhon MS, Ainslie PN, Griesdale DE. Clinical pathophysiology of hypoxic ischemic brain injury after cardiac arrest: a "two-hit" model. *Critical Care (London, England)*. 2017;21:90. doi: [10.1186/s13054-017-1670-9](https://doi.org/10.1186/s13054-017-1670-9)
- Drabek T, Foley LM, Janata A, Stezoski J, Kevin Hitchens T, Manole MD, Kochanek PM. Global and regional differences in cerebral blood flow after asphyxial versus ventricular fibrillation cardiac arrest in rats using ASL-MRI. *Resuscitation*. 2014;85:964–971. doi: [10.1016/j.resuscitation.2014.03.314](https://doi.org/10.1016/j.resuscitation.2014.03.314)
- Gong P, Zhao S, Wang J, Yang Z, Qian J, Wu X, Cahoon J, Tang W. Mild hypothermia preserves cerebral cortex microcirculation after resuscitation in a rat model of cardiac arrest. *Resuscitation*. 2015;97:109–114. doi: [10.1016/j.resuscitation.2015.10.003](https://doi.org/10.1016/j.resuscitation.2015.10.003)
- Wang CH, Chang WT, Huang CH, Tsai MS, Liu SH, Chen WJ. Cerebral blood flow-guided manipulation of arterial blood pressure attenuates hippocampal apoptosis after asphyxia-induced cardiac arrest in rats. *J Am Heart Assoc*. 2020;9:e016513. doi: [10.1161/jaha.120.016513](https://doi.org/10.1161/jaha.120.016513)
- Babini G, Ristagno G, Boccardo A, De Giorgio D, De Maglie M, Affatato R, Ceriani S, Zani D, Novelli D, Staszewsky L, et al. Effect of mild hypercapnia on outcome and histological injury in a porcine post cardiac arrest model. *Resuscitation*. 2019;135:110–117. doi: [10.1016/j.resuscitation.2018.10.024](https://doi.org/10.1016/j.resuscitation.2018.10.024)

10. Zhou Q, Cao B, Niu L, Cui X, Yu H, Liu J, Li H, Li W. Effects of permissive hypercapnia on transient global cerebral ischemia-reperfusion injury in rats. *Anesthesiology*. 2010;112:288–297. doi: [10.1097/ALN.0b013e318ca8257](https://doi.org/10.1097/ALN.0b013e318ca8257)
11. Tao T, Liu Y, Zhang J, Xu Y, Li W, Zhao M. Therapeutic hypercapnia improves functional recovery and attenuates injury via antiapoptotic mechanisms in a rat focal cerebral ischemia/reperfusion model. *Brain Res*. 2013;1533:52–62. doi: [10.1016/j.brainres.2013.08.014](https://doi.org/10.1016/j.brainres.2013.08.014)
12. Cui D, Shang H, Zhang X, Jiang W, Jia X. Cardiac arrest triggers hippocampal neuronal death through autophagic and apoptotic pathways. *Sci Rep*. 2016;6:27642. doi: [10.1038/srep27642](https://doi.org/10.1038/srep27642)
13. Percie du Sert N, Hurst V, Ahluwalia A, Alam S, Avey MT, Baker M, Browne WJ, Clark A, Cuthill IC, Dirnagl U, et al. The ARRIVE guidelines 2.0: updated guidelines for reporting animal research. *PLoS Biol*. 2020;18:e3000410. doi: [10.1371/journal.pbio.3000410](https://doi.org/10.1371/journal.pbio.3000410)
14. Wang CH, Chang WT, Tsai MS, Huang CH, Chen WJ. Synergistic effects of moderate therapeutic hypothermia and levosimendan on cardiac function and survival after asphyxia-induced cardiac arrest in rats. *J Am Heart Assoc*. 2020;9:e016139. doi: [10.1161/jaha.120.016139](https://doi.org/10.1161/jaha.120.016139)
15. Nishijima T, Okamoto M, Matsui T, Kita I, Soya H. Hippocampal functional hyperemia mediated by NMDA receptor/NO signaling in rats during mild exercise. *J Appl Physiol (1985)*. 2012;112:197–203. doi: [10.1152/jappphysiol.00763.2011](https://doi.org/10.1152/jappphysiol.00763.2011)
16. Abella BS, Zhao D, Alvarado J, Hamann K, Vanden Hoek TL, Becker LB. Intra-arrest cooling improves outcomes in a murine cardiac arrest model. *Circulation*. 2004;109:2786–2791. doi: [10.1161/01.cir.0000131940.19833.85](https://doi.org/10.1161/01.cir.0000131940.19833.85)
17. Dolenc P, Pilipovic K, Rajic J, Zupan G. Temporal pattern of neurodegeneration, programmed cell death, and neuroplastic responses in the thalamus after lateral fluid percussion brain injury in the rat. *J Neuropathol Exp Neurol*. 2015;74:512–526. doi: [10.1097/nen.0000000000000194](https://doi.org/10.1097/nen.0000000000000194)
18. Marina N, Christie IN, Korsak A, Doronin M, Brazhe A, Hosford PS, Wells JA, Sheikhabahaei S, Humoud I, Paton JFR, et al. Astrocytes monitor cerebral perfusion and control systemic circulation to maintain brain blood flow. *Nat Commun*. 2020;11:131. doi: [10.1038/s41467-019-13956-y](https://doi.org/10.1038/s41467-019-13956-y)
19. Christopherson TJ, Milde JH, Michenfelder JD. Cerebral vascular autoregulation and CO₂ reactivity following onset of the delayed postischemic hypoperfusion state in dogs. *J Cereb Blood Flow Metab*. 1993;13:260–268. doi: [10.1038/jcbfm.1993.32](https://doi.org/10.1038/jcbfm.1993.32)
20. Bottiger BW, Krumnikl JJ, Gass P, Schmitz B, Motsch J, Martin E. The cerebral 'no-reflow' phenomenon after cardiac arrest in rats—Influence of low-flow reperfusion. *Resuscitation*. 1997;34:79–87. doi: [10.1016/s0300-9572\(96\)01029-5](https://doi.org/10.1016/s0300-9572(96)01029-5)
21. Ames A III, Wright RL, Kowada M, Thurston J, Majno G. Cerebral ischemia. II. The no-reflow phenomenon. *Am J Pathol*. 1968;52:437–453.
22. Cingolani HE, Mattiazzi AR, Blesa ES, Gonzalez NC. Contractility in isolated mammalian heart muscle after acid-base changes. *Circ Res*. 1970;26:269–278. doi: [10.1161/01.RES.26.3.269](https://doi.org/10.1161/01.RES.26.3.269)
23. Houle DB, Weil MH, Brown EB Jr, Campbell GS. Influence of respiratory acidosis on ECG and pressor responses to epinephrine, norepinephrine and metaraminol. *Proc Soc Exp Biol Med*. 1957;94:561–564. doi: [10.3181/00379727-94-23012](https://doi.org/10.3181/00379727-94-23012)
24. Wang CH, Chang WT, Huang CH, Tsai MS, Yu PH, Wu YW, Chen WJ. Associations between early intra-arrest blood acidemia and outcomes of adult in-hospital cardiac arrest: a retrospective cohort study. *J Formos Med Assoc*. 2019;119:644–651. doi: [10.1016/j.jfma.2019.08.020](https://doi.org/10.1016/j.jfma.2019.08.020)
25. Abu Romeh S, Tannen RL. Amelioration of hypoxia-induced lactic acidosis by superimposed hypercapnea or hydrochloric acid infusion. *Am J Physiol*. 1986;250:F702–F709. doi: [10.1152/ajprenal.1986.250.4.F702](https://doi.org/10.1152/ajprenal.1986.250.4.F702)
26. Nomura F, Aoki M, Forbess JM, Mayer JE Jr. Effects of hypercarbic acidotic reperfusion on recovery of myocardial function after cardioplegic ischemia in neonatal lambs. *Circulation*. 1994;90:11321–11327.
27. Li AM, Quan Y, Guo YP, Li WZ, Cui XG. Effects of therapeutic hypercapnia on inflammation and apoptosis after hepatic ischemia-reperfusion injury in rats. *Chin Med J (Engl)*. 2010;123:2254–2258.
28. Wang CH, Chang WT, Huang CH, Tsai MS, Yu PH, Wang AY, Chen NC, Chen WJ. The effect of hyperoxia on survival following adult cardiac arrest: a systematic review and meta-analysis of observational studies. *Resuscitation*. 2014;85:1142–1148. doi: [10.1016/j.resuscit.2014.05.021](https://doi.org/10.1016/j.resuscit.2014.05.021)
29. Wang CH, Huang CH, Chang WT, Tsai MS, Lu TC, Yu PH, Wang AY, Chen NC, Chen WJ. Association between early arterial blood gas tensions and neurological outcome in adult patients following in-hospital cardiac arrest. *Resuscitation*. 2015;89:1–7. doi: [10.1016/j.resuscit.2015.01.003](https://doi.org/10.1016/j.resuscit.2015.01.003)
30. Marquez AM, Morgan RW, Ko T, Landis WP, Hefti MM, Mavroudis CD, McManus MJ, Karlsson M, Starr J, Roberts AL, et al. Oxygen exposure during cardiopulmonary resuscitation is associated with cerebral oxidative injury in a randomized, blinded, controlled, preclinical trial. *J Am Heart Assoc*. 2020;9:e015032. doi: [10.1161/jaha.119.015032](https://doi.org/10.1161/jaha.119.015032)
31. Liu Y, Rosenthal RE, Haywood Y, Miljkovic-Lolic M, Vanderhoeck JY, Fiskum G. Normoxic ventilation after cardiac arrest reduces oxidation of brain lipids and improves neurological outcome. *Stroke*. 1998;29:1679–1686. doi: [10.1161/01.STR.29.8.1679](https://doi.org/10.1161/01.STR.29.8.1679)
32. Jakkula P, Reinikainen M, Hastbacka J, Loisa P, Tiainen M, Pettila V, Toppila J, Lahde M, Backlund M, Okkonen M, et al. Targeting two different levels of both arterial carbon dioxide and arterial oxygen after cardiac arrest and resuscitation: a randomised pilot trial. *Intensive Care Med*. 2018;44:2112–2121. doi: [10.1007/s00134-018-5453-9](https://doi.org/10.1007/s00134-018-5453-9)
33. Wang CH, Chang WT, Su KI, Huang CH, Tsai MS, Chou E, Lu TC, Chen WJ, Lee CC, Chen SC. Neuroprognostic accuracy of blood biomarkers for post-cardiac arrest patients: a systematic review and meta-analysis. *Resuscitation*. 2020;148:108–117. doi: [10.1016/j.resuscit.2020.01.006](https://doi.org/10.1016/j.resuscit.2020.01.006)
34. Redza-Dutordoir M, Averill-Bates DA. Activation of apoptosis signalling pathways by reactive oxygen species. *Biochim Biophys Acta*. 2016;1863:2977–2992. doi: [10.1016/j.bbamcr.2016.09.012](https://doi.org/10.1016/j.bbamcr.2016.09.012)
35. Agarwal A, Mahfouz RZ, Sharma RK, Sarkar O, Mangrola D, Mathur PP. Potential biological role of poly (ADP-ribose) polymerase (PARP) in male gametes. *Reprod Biol Endocrinol*. 2009;7:143. doi: [10.1186/1477-7827-7-143](https://doi.org/10.1186/1477-7827-7-143)
36. Salvesen GS, Dixit VM. Caspases: intracellular signaling by proteolysis. *Cell*. 1997;91:443–446. doi: [10.1016/s0092-8674\(00\)80430-4](https://doi.org/10.1016/s0092-8674(00)80430-4)
37. Tewari M, Quan LT, O'Rourke K, Desnoyers S, Zeng Z, Beidler DR, Poirier GG, Salvesen GS, Dixit VM. Yama/CPP32 beta, a mammalian homolog of CED-3, is a CrmA-inhibitable protease that cleaves the death substrate poly(ADP-ribose) polymerase. *Cell*. 1995;81:801–809. doi: [10.1016/0092-8674\(95\)90541-3](https://doi.org/10.1016/0092-8674(95)90541-3)
38. Lin L, Baehrecke EH. Autophagy, cell death, and cancer. *Mol Cell Oncol*. 2015;2:e985913. doi: [10.4161/23723556.2014.985913](https://doi.org/10.4161/23723556.2014.985913)
39. Chatterjee S, Sarkar S, Bhattacharya S. Toxic metals and autophagy. *Chem Res Toxicol*. 2014;27:1887–1900. doi: [10.1021/tx500264s](https://doi.org/10.1021/tx500264s)
40. Liu WJ, Ye L, Huang WF, Guo LJ, Xu ZG, Wu HL, Yang C, Liu HF. p62 links the autophagy pathway and the ubiquitin-proteasome system upon ubiquitinated protein degradation. *Cell Mol Biol Lett*. 2016;21:29. doi: [10.1186/s11658-016-0031-z](https://doi.org/10.1186/s11658-016-0031-z)
41. Goodall ML, Fitzwalter BE, Zahedi S, Wu M, Rodriguez D, Mulcahy-Levy JM, Green DR, Morgan M, Cramer SD, Thorburn A. The autophagy machinery controls cell death switching between apoptosis and necroptosis. *Dev Cell*. 2016;37:337–349. doi: [10.1016/j.devcel.2016.04.018](https://doi.org/10.1016/j.devcel.2016.04.018)
42. Holmberg MJ, Nicholson T, Nolan JP, Schexnayder S, Reynolds J, Nattion K, Welsford M, Morley P, Soar J, Berg KM. Oxygenation and ventilation targets after cardiac arrest: a systematic review and meta-analysis. *Resuscitation*. 2020;152:107–115. doi: [10.1016/j.resuscit.2020.04.031](https://doi.org/10.1016/j.resuscit.2020.04.031)
43. Eastwood GM, Schneider AG, Suzuki S, Peck L, Young H, Tanaka A, Mårtensson J, Warrillow S, McGuinness S, Parke R, et al. Targeted therapeutic mild hypercapnia after cardiac arrest: a phase II multi-centre randomised controlled trial (the CCC trial). *Resuscitation*. 2016;104:83–90. doi: [10.1016/j.resuscitation.2016.03.023](https://doi.org/10.1016/j.resuscitation.2016.03.023)
44. Wihersaari L, Ashton NJ, Reinikainen M, Jakkula P, Pettilä V, Hästbacka J, Tiainen M, Loisa P, Friberg H, Cronberg T, et al. Neurofilament light as an outcome predictor after cardiac arrest: a post hoc analysis of the COMACARE trial. *Intensive Care Med*. 2021;47:39–48. doi: [10.1007/s00134-020-06218-9](https://doi.org/10.1007/s00134-020-06218-9)
45. Panchal AR, Bartos JA, Cabañas JG, Donnino MW, Drennan IR, Hirsch KG, Kudenchuk PJ, Kurz MC, Lavonas EJ, Morley PT, et al. Part 3: adult basic and advanced life support: 2020 American heart association guidelines for cardiopulmonary resuscitation and emergency cardiovascular care. *Circulation*. 2020;142:S366–S468. doi: [10.1161/cir.0000000000000916](https://doi.org/10.1161/cir.0000000000000916)
46. Nolan JP, Sandroni C, Böttiger BW, Cariou A, Cronberg T, Friberg H, Genbrugge C, Haywood K, Lijja G, Moulart VRM, et al. European resuscitation council and European Society of Intensive Care Medicine guidelines 2021: post-resuscitation care. *Resuscitation*. 2021;161:220–269. doi: [10.1016/j.resuscitation.2021.02.012](https://doi.org/10.1016/j.resuscitation.2021.02.012)

SUPPLEMENTAL MATERIAL

Table S1. Neurological function score (NFS) definitions.

Level of consciousness	Corneal reflex	Respiration	Righting reflex	Coordination	Movement/ activity	Score
No reaction to tail pinching	No blinking	Irregular breathing pattern	No turning attempts	No movement	No spontaneous movement	0
Poor response to tail pinching	Sluggish blinking	Decreased breathing frequency, normal pattern	Sluggish turning	Moderate ataxia	Sluggish movement	1
Normal response to tail pinching	Normal blinking	Normal breathing frequency and pattern	Turns over quickly and spontaneously	Normal coordination	Normal movement	2

Figure S1. Flow diagram showing randomization and testing procedures. CA, cardiac arrest; CPR, cardiopulmonary resuscitation; ROSC, return of spontaneous circulation.

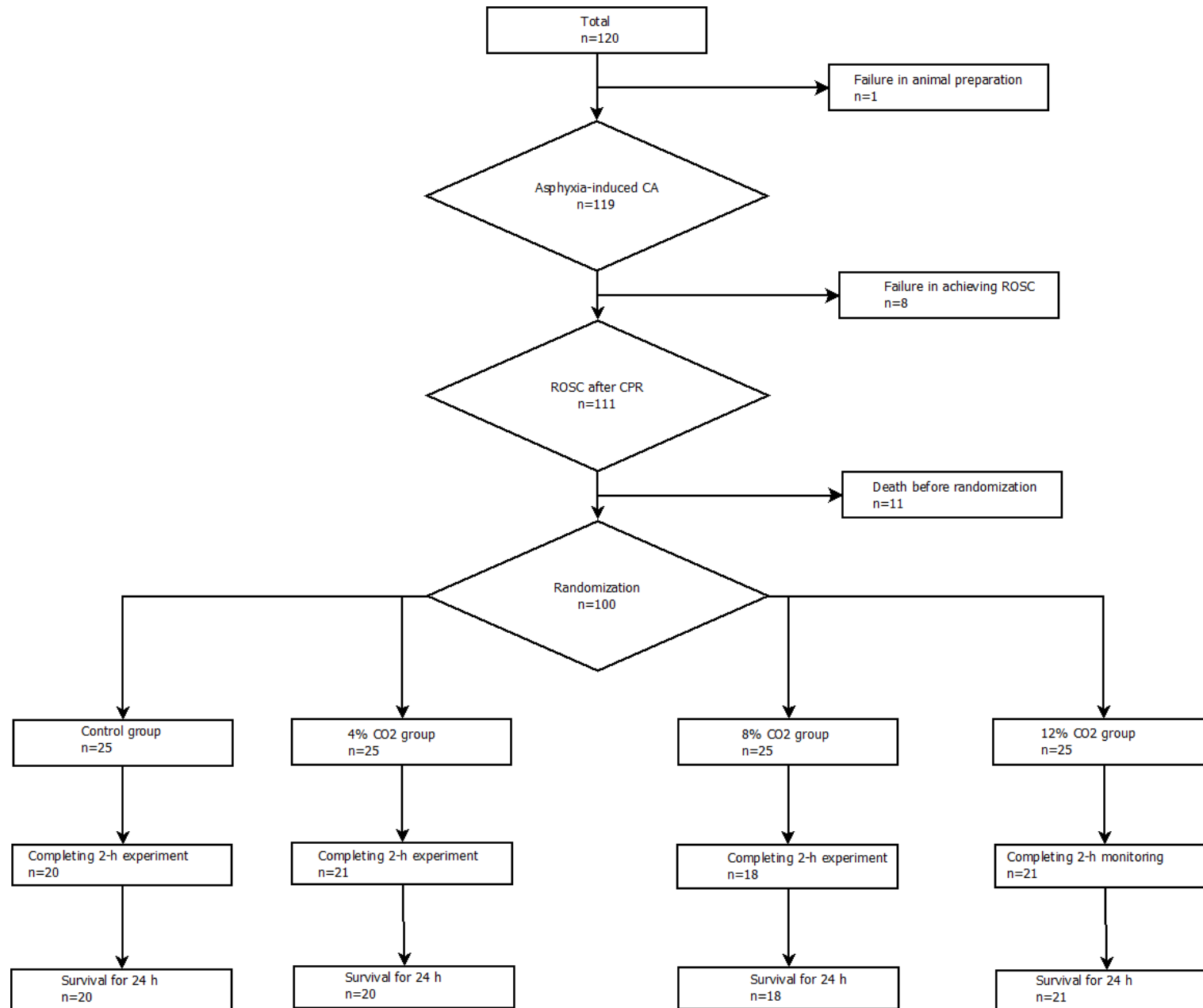


Figure S2. Survival curves in control and experimental groups.

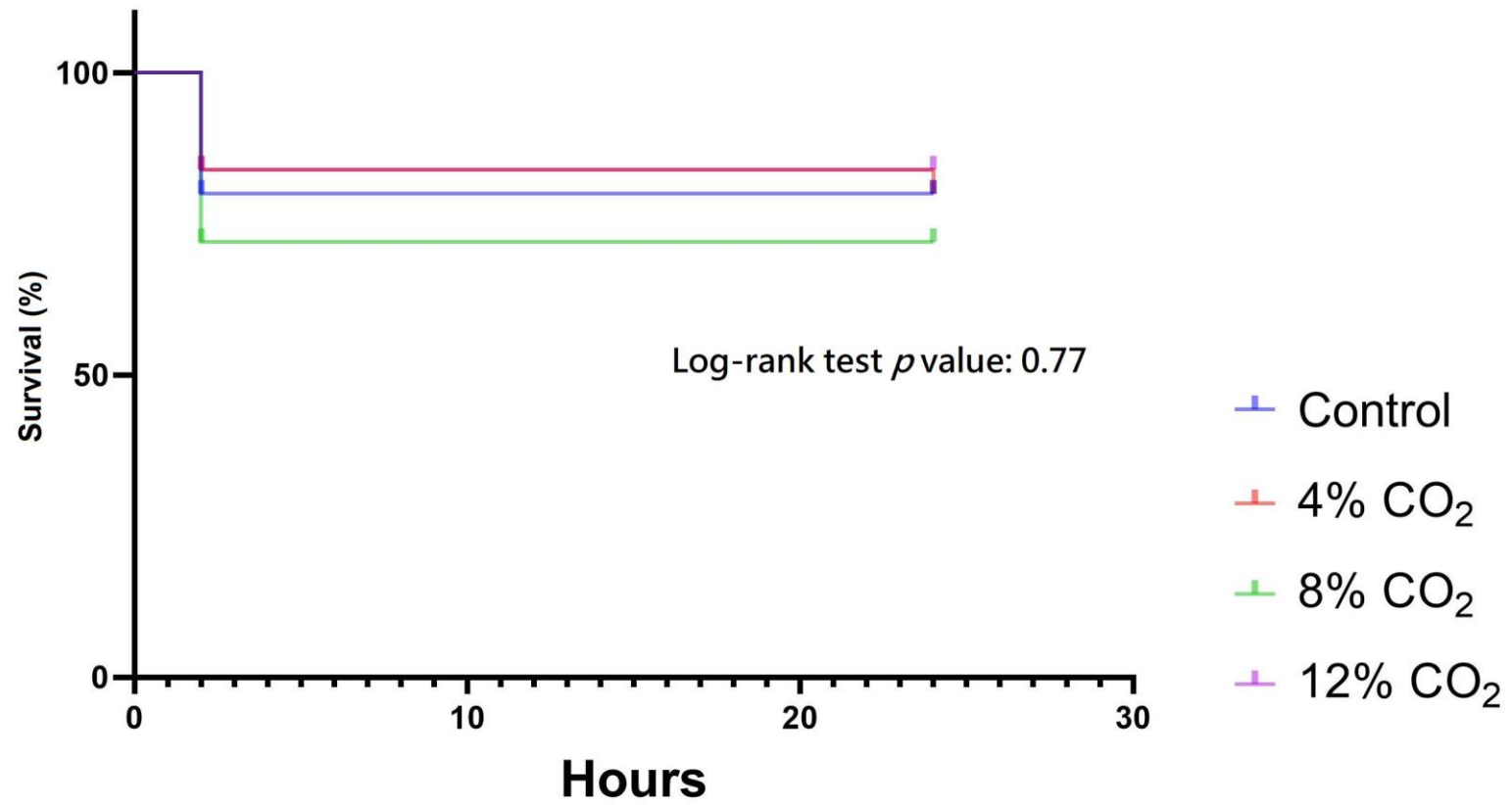
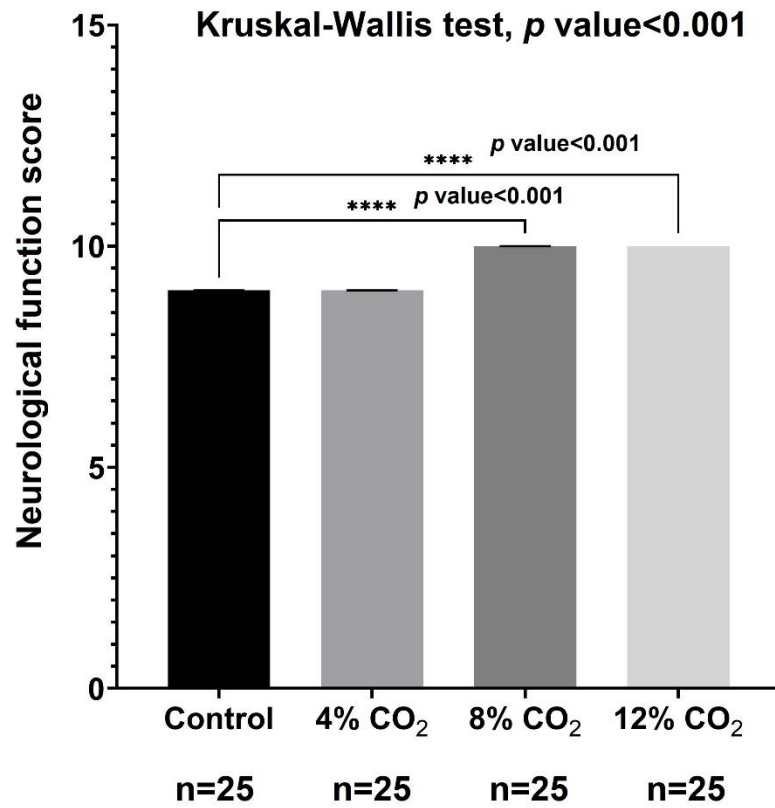


Figure S3. Sensitivity analysis comparing neurological outcomes at 24 h post-ROSC in (A) best scenario; and (B) worst scenario. These results suggest that the comparison in neurological function score was robust after accounting for the influence of the rats with early death.

(A)



(B)

